SLAC-PUB-16249

DESIGN OF A 6 TEV MUON COLLIDER

M-H. Wang, Y. Nosochkov, Y. Cai

SLAC, 2575 Sand Hill Road, Menlo Park, CA 94025, USA

M. Palmer

FNAL, P.O. Box 500, Batavia, IL 60510, USA

Abstract

A preliminary design of a muon collider ring with the center of mass (CM) energy of 6 TeV is presented. The ring circumference is 6.3 km, and the β functions at collision point are 1 cm in each plane. The ring linear optics, the non-linear chromaticity compensation in the Interaction Region (IR), and the additional non-linear orthogonal correcting knobs are described. Magnet specifications are based on the maximum pole-tip field of 20T in dipoles and 15T in quadrupoles. Careful compensation of the non-linear chromatic and amplitude dependent effects provide a sufficiently large dynamic aperture for the momentum range of up to ±0.5% without considering magnet errors.

INTRODUCTION

A muon collider is one of the potential candidates for a future energy frontier colliding machine. Considering requirements on energy, luminosity and wall power in operation, the preferred choice of the center of mass muon beam energy appears to be near 6 TeV [1]. In order to obtain peak luminosity of $\geq 10^{34}$ $cm^{-2}s^{-1}$ in the TeV range, a number of demanding requirements to the collider optics should be satisfied [2]. The requirements are arising from a short muon lifetime and relatively large values of transverse emittance and momentum spread that can be realistically achieved with ionization cooling. The requirements also come from the limitations on the maximum magnetic operating fields as well as the necessity to protect superconducting (SC) magnets and collider detectors from muon decay products. Another complication associated with high muon energy is the "hot spots" of radiation which can be induced by neutrinos from muon decay in straight sections [3]. As a result, straight sections without bending field must be very short.

Some of the important requirements for the muon collider lattice are listed below [2]:

• Low β function ($\leq$ 1cm) at the Interaction Point (IP) resulting in extremely large beta functions in the IR final focusing (FF) quadrupoles.

• Small circumference C providing a high revolution frequency. This, however, implies strong magnetic field and small to moderate magnet aperture.

• Sufficiently large dynamic aperture for the expected normalized beam emittance of ~25 μm-rad, and momentum acceptance of up to 1%.

• Low momentum compaction factor ($\alpha_c < 10^{-4}$) for a short bunch length $\sigma_z \leq \beta^*$ and reasonable RF voltage $U_{RF} < 1$ GV.

• Absence of long straights to avoid hot spots of neutrino radiation. This requires weak dipoles in most of the straights.

• Protection of the FF quadrupoles and the IR detector from secondary particles. This leads to a limitation to the FF quadrupole field gradient and quadrupole distance from the IP.

This material is based upon work supported by the U.S. Department of Energy, Office of Science, Office of Basic Energy Sciences, under Contract No. DE-AC02-76SF00515 and HEP.

• Acceptable sensitivity to machine errors which limits the maximum values of β-functions in the magnets.

LINEAR OPTICS

For a 6 TeV muon collider ring, achieving a short circumference and strong focusing in the IR requires rather high magnetic field. In this design, we chose the circumference of ≈6.3 km (approximately the size of the Tevatron) and the maximum pole-tip field of 20T in dipoles and 15T in quadrupoles. We expect that future advances in SC magnet design will make achieving such a strong field possible. The designed ring lattice has a two-fold symmetry (periodicity) and consists of two identical IRs and two arcs.

Interaction Region

Interaction region is the most challenging part of a high luminosity collider due to the extremely high beta functions in the FF quadrupoles generating large non-linear chromaticity as well as resulting in high sensitivity to machine errors. The designed optics of one half of the IR of the 6 TeV machine is shown in Fig. 1, where IP is on the left-hand side with $\beta^* = 1$ cm in *x* and *y* planes. The IP is followed by a 6 m free space and a final focusing quadrupole doublet where vertical beta function reaches an extremely high value of 134 km. The remaining part of the IR is made of FODO-like lattice where most of the space between the quadrupoles is filled with dipole magnets to avoid hot spots of neutrino radiation. Due to the high beta functions, the FF quadrupoles generate very large non-linear chromaticity resulting in a non-linear chromatic tune shift and large energy dependent perturbation of beta functions. These effects must be locally compensated to avoid a severe degradation of the ring momentum acceptance. The designed IR chromaticity correction scheme is based on two (*x* and *y*) non-interleaved pairs of sextupoles on each side of the IP, where the sextupoles in each pair are separated by –I transformation for cancellation of the 2nd order sextupole geometric (amplitude dependent) aberrations. The sextupoles are placed near the high beta peaks (*x* and *y*) to maximize their effective strengths as one can see in Fig.1. This scheme will be discussed in more detail later. The FODO cells at each end of the IR are designed for cancellation of dispersion, followed by ~40 m of non-dispersive region. The latter can be used for beam injection, placement of RF-cavities as well as geometric (harmonic) sextupoles or octupoles for additional non-linear compensation. On the right-hand side of Fig.1, the IR is followed by the arc dispersion suppressor which matches the IR optics to the periodic arc.

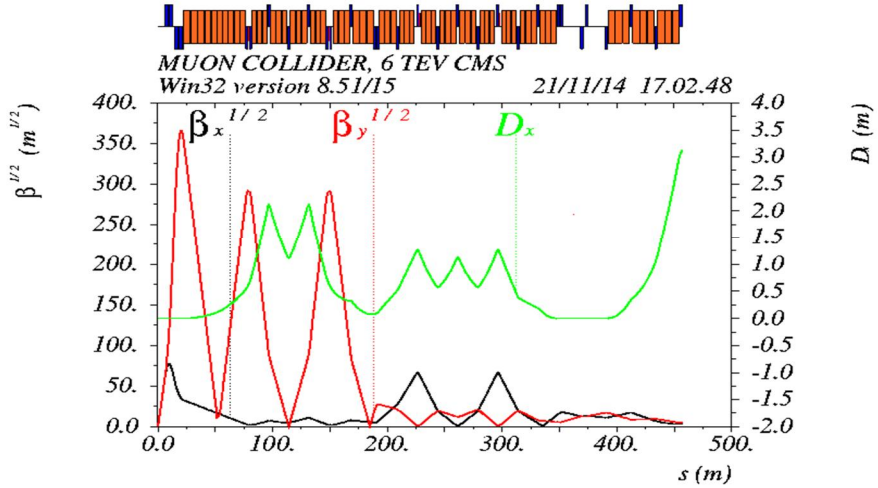

Figure 1. Linear optics of one half of the IR and the arc dispersion suppressor, where β* = 1 cm at the IP (on the left-hand side), and the detector free space is L* = 6 m. Two –I pairs of sextupoles (*x* and *y*) are placed at large β_y and β_x peaks for local correction of the FF quadrupole non-linear chromaticity.

Arcs

The arc lattice of the 6 TeV ring is based on the arc lattice design for the 1.5 TeV muon collider (by Y. Alexahin [4]). The 6 TeV arc cell has the same length as in the 1.5 TeV design, but due to the longer circumference the bending angle per cell in the 6 TeV ring is reduced, and the number of cells per each arc is increased from 6 to 16. Each cell contains three sextupole families for correction of linear chromaticity. Phase advance per arc cell is changed from the original $\mu_x/\mu_y = 0.833/0.833$ [2π] to 0.875/0.875 [2π]. The latter provides a unit transformation per each half arc leading to local cancellation of most of the sextupole non-linear geometric aberrations. The magnet pole-tip field is increased with the higher energy, but is kept below 15T in quadrupoles and 20T in dipoles. Optics functions of one arc cell are shown in Fig. 2. The complete ring optics is presented in Fig. 3.

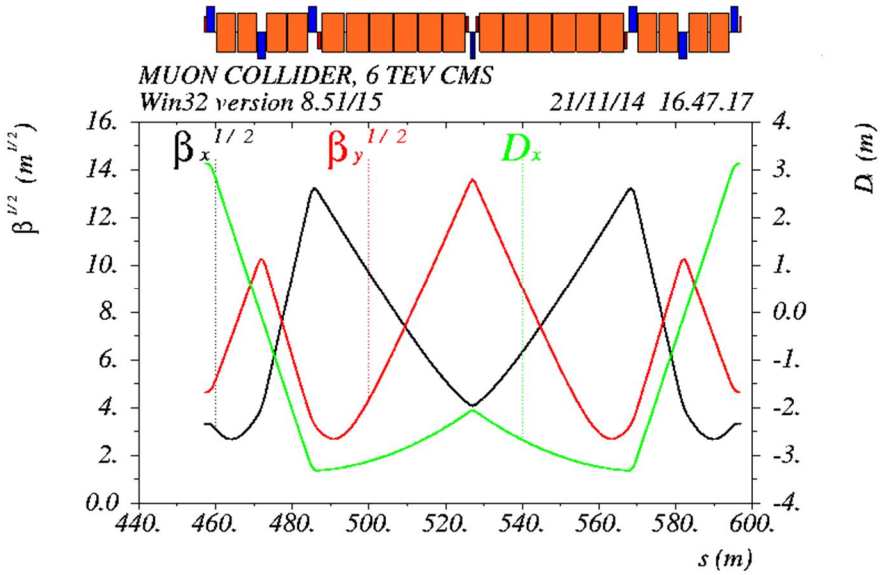

Figure 2. Linear optics of one arc cell, where phase advance per cell is 0.875/0.875 [2π]. Each arc contains 16 cells providing a unit transformation per each half arc.

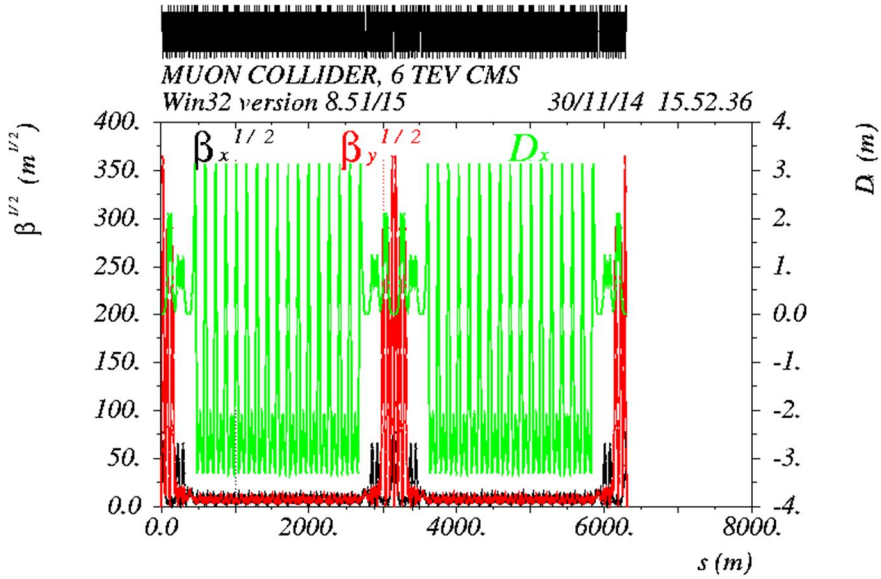

Figure 3. Linear optics of the complete 6 TeV muon collider. The ring has a two-fold symmetry (periodicity), circumference of ≈6.3 km, and betatron tune of $\nu_x/\nu_y = 38.23/40.14$.

IR Magnet Parameters

The IR magnets must provide sufficient aperture for the beam while satisfying the limitation on the pole-tip field described earlier. The minimum half-aperture in the IR magnets is specified based on the definition of $5\sigma_{x,y}$ + 15 mm, where the 15 mm is a contingency for hardware including cryogenic cooling channel [5]. The required minimum half-aperture corresponding to the normalized beam emittance of 25 mm-mrad and rms energy spread of 0.1% is shown in Fig. 4. Due to the limitation on the pole-tip field, the large aperture in the FF quadrupole doublet leads to a relatively weak gradient, therefore long FF quadrupoles are needed to provide the necessary strength. To minimize the FF length, the doublet quadrupoles are divided into shorter magnets where the individual quadrupole apertures are adjusted according to the rapidly changing beta functions in this area. This reduces the required magnet aperture where beta functions are lower, thus increasing the corresponding quadrupole gradient and reducing the total quadrupole length. Apertures of the other IR quadrupoles are divided into three groups depending on their beta functions. The resulting IR magnet specifications are presented in Table 1.

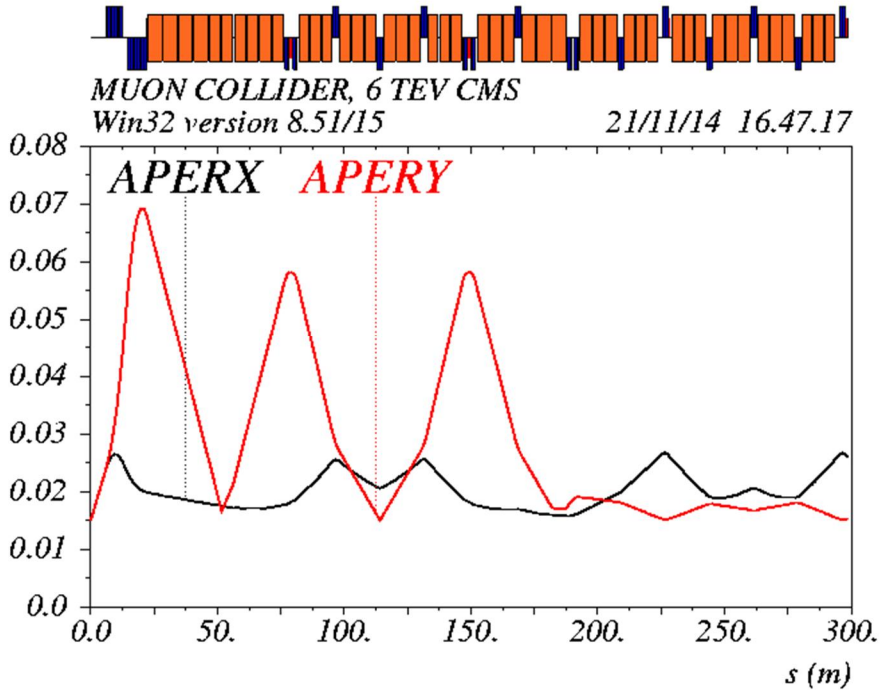

Figure 4. Minimum half-aperture of the IR magnets based on the definition of $5\sigma_{x,y}$ + 15 mm.

Table 1. IR magnet parameters for the 6 TeV design.

Magnet	Half-aperture (mm)	Pole-tip field (T)	Length (m)
QIR01A	30	14.52	1.85
QIR01B	35	14.52	1.85
QIR01C	45	14.52	1.85
QIR02A	65	-14.94	2.2
QIR02B	75	-14.94	2.2
QIR02C	75	-14.94	2.2

QIR#	60, 30, 25	< 15	2.0 (1.7 for QIR03,07)
Dipole	50 (66)	< 20	4/4.5/5.5

The main parameters of the 6 TeV ring are listed in Table 2. For comparison, parameters of the earlier designs for 1.5 TeV [6] and 3 TeV [7] CM energy are shown as well. Note that the luminosity values of the 3 TeV and 6 TeV designs in Table 2 do not include the beam-beam and the hourglass effects at IP; and they should not be considered as "official" values.

Table 2. Comparison of the 6 TeV ring parameters with the earlier designs for 1.5 and 3 TeV.

Parameter	Unit	1.5 TeV design [6]	3 TeV design [7]	6 TeV design
Beam energy	TeV	0.75	1.5	3.0
Number of IPs		2	2	2
Circumference	m	2730	2767	6302
β*	cm	1	1	1
Tune x/y		18.56/16.58	20.13/22.22	38.23/40.14
Momentum compaction		-1.30E-5	-2.88E-4	-1.216E-3
Normalized emittance	mm·mrad	25	25	25
Momentum spread	%	0.1	0.1	0.1
Bunch length	cm	1	1	1
Muons/bunch	10^{12}	2	2	2
Repetition rate	Hz	15	15	15
Average luminosity	10^{34} cm^{-2}s^{-1}	1.1	4.5	7.1

CHROMATICITY CORRECTION

Chromaticity of a collider with low IP beta functions is dominated by the FF quadrupoles. Due to the extremely high beta functions, these quadrupoles generate not only a significant part of linear chromaticity, but also are the main source of non-linear chromaticity such as a non-linear chromatic tune shift and energy dependent perturbation of beta functions. These non-linear effects must be compensated to avoid the chromatic perturbation to propagating around the ring, thus further increasing the non-linear effects and severely limiting the ring momentum acceptance. This requires a dedicated local correction system using sextupoles in the IR. The included IR chromaticity correction scheme is based on two non-interleaved pairs of sextupoles (SIRY1-SIRY2 and SIRX1-SIRX2) for *x* and *y* correction on each side of IP, where the sextupoles in each pair are separated by –I transformation for cancellation of the 2nd order sextupole geometric (amplitude dependent) aberrations. To provide an efficient correction of the FF chromaticity, the following conditions at the sextupoles are implemented: 1) sufficiently large dispersion and very large beta function to provide a required sextupole effect with a limited sextupole magnetic field; 2) large β_x/β_y or β_y/β_x ratio for orthogonal *x* and *y* correction; 3) nπ phase advance (in the correcting plane) between the FF quads and the sextupoles; 4) no other quadrupoles between the FF doublet and the first sextupole to avoid chromatic

perturbation of phase advance between them. The sextupoles are located near the high beta peaks (*y* and *x*) as can be seen in Fig.1.

The remaining linear chromaticity of the machine (after the IR correction) can be canceled using three families of sextupoles in the periodic arc cells. These sextupoles are arranged in a way that cancels many of the sextupole driven non-linear effects locally in each arc. This is made possible by choosing an optimal cell phase advance of 0.875/0.875 [2π]. The resulting +I transformation in each half arc (8 periodic cells) makes the latter an almost exact fourth order geometric achromat [8, 9]. The remaining non-vanishing effects of the arc sextupoles are the resonance driving term $2\nu_x - 2\nu_y$ and five phase independent terms: two second order chromatic tune terms and three amplitude dependent tune terms.

The initial set-up of the IR and the arc sextupole strengths was performed in MAD [10] using the following method. First, the IR sextupole strengths were adjusted to locally cancel the *x* and *y* W-functions [10] at the IP as shown in Fig. 5. This way, the chromatic variation of IP beta functions and, therefore, the IP beam size, are minimized. At the same time, the second order terms of the chromatic tune shift generated by the FF quadrupoles are compensated as well. As a second step, the remaining ring linear chromaticity is cancelled using the three sextupole families in the arcs. This two-step procedure can be used iteratively, if needed, to obtain simultaneous cancellation of the IP W-functions and the ring linear chromaticity. The effect of this compensation on beam dynamic aperture was verified in tracking simulations using LEGO [11] for machine without magnet errors. Fig. 6 shows the dynamic aperture at IP for on and off-momentum particles up to $\Delta p/p = 0.4\%$. The tune footprint, the amplitude dependent tunes, and the chromatic tune shifts derived from the tracking data are shown in Fig. 7-9. One can see that the vertical dynamic aperture is rather poor (about $2\sigma_y$), and the momentum range is limited to $\Delta p/p = 0.4\%$. Fig. 8, 9 reveal that the vertical amplitude dependent tune shift and the horizontal chromatic tune shift are large. Therefore, further non-linear compensation is required in order to reduce these effects. The goal of the additional non-linear compensation is to increase the *x* and *y* dynamic aperture to more than 5σ, where σ = 3 μm (at IP) at 3 TeV energy per beam, and increase the momentum range to at least ±0.5%.

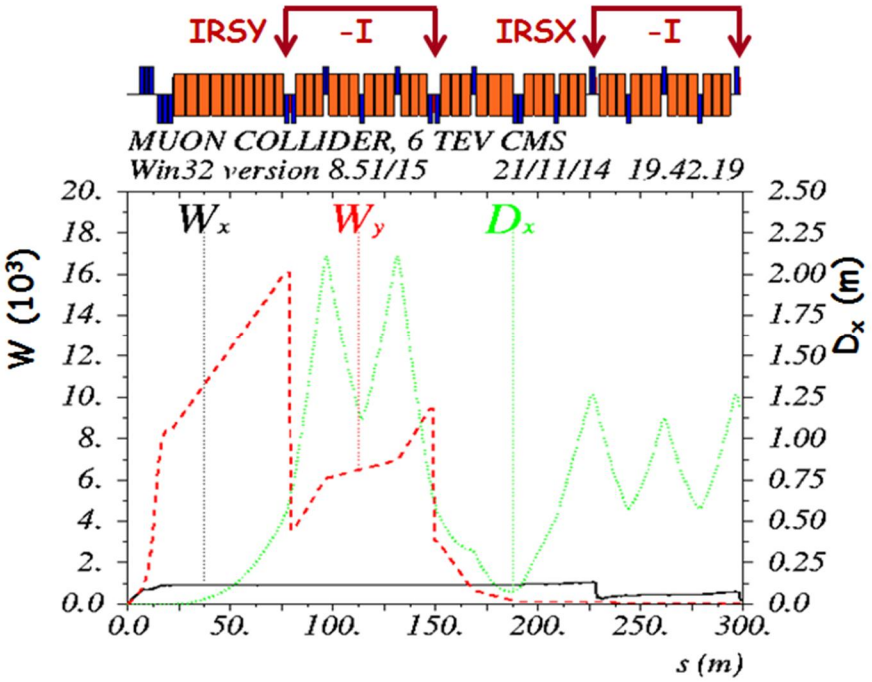

Figure 5. W-functions are locally cancelled at the IP (S = 0) and outside of the IR using the –I

sextupole pairs. The remaining linear chromaticity in the ring is canceled using arc sextupoles.

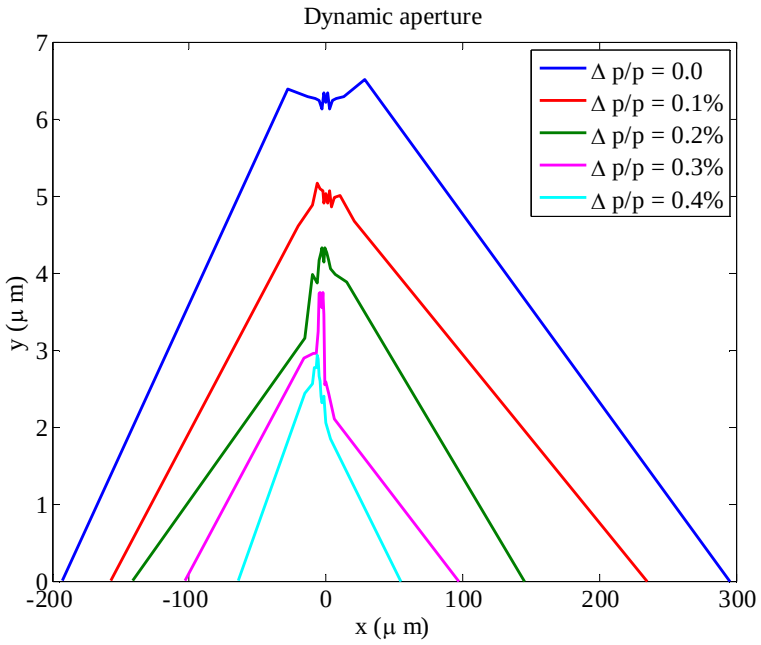

Figure 6. Dynamic aperture at IP for the ring with IR local sextupole pairs and three families of arc sextupoles. The vertical aperture is not sufficient, and the momentum range is below 0.5%.

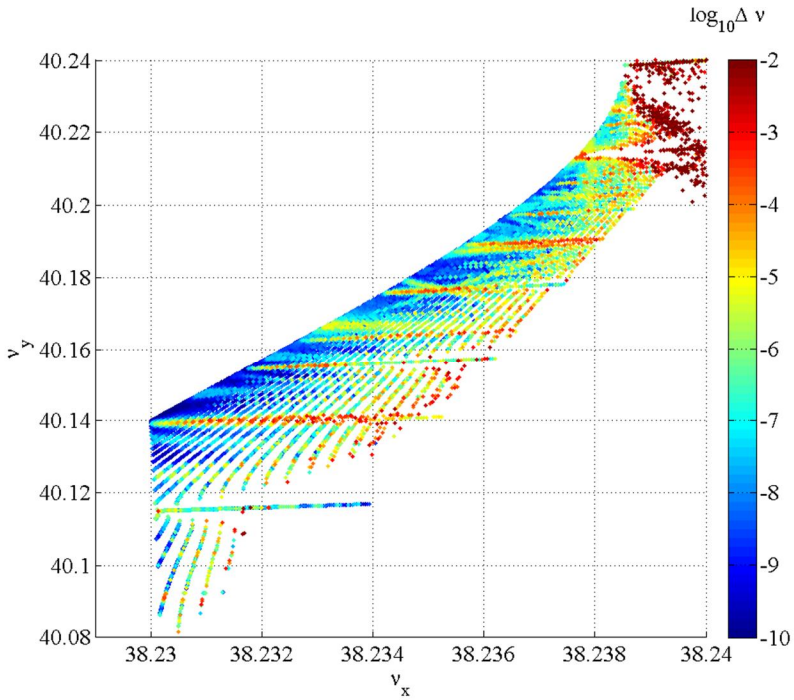

Figure 7. Tune footprint for the ring with IR local sextupole pairs and three families of arc sextupoles.

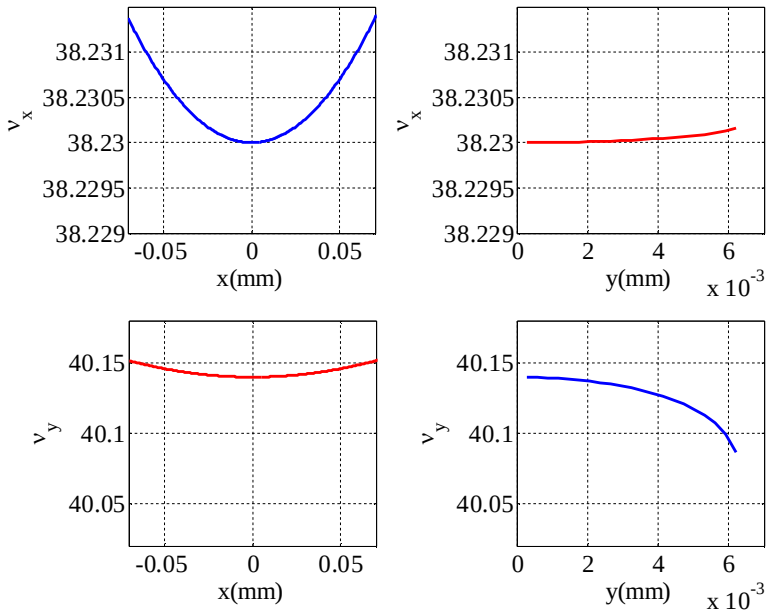

Figure 8. Tune shift with amplitude for the ring with IR local sextupole pairs and three families of arc sextupoles. The vertical amplitude drives the vertical tune towards the integer resonance, thus limiting the vertical dynamic aperture.

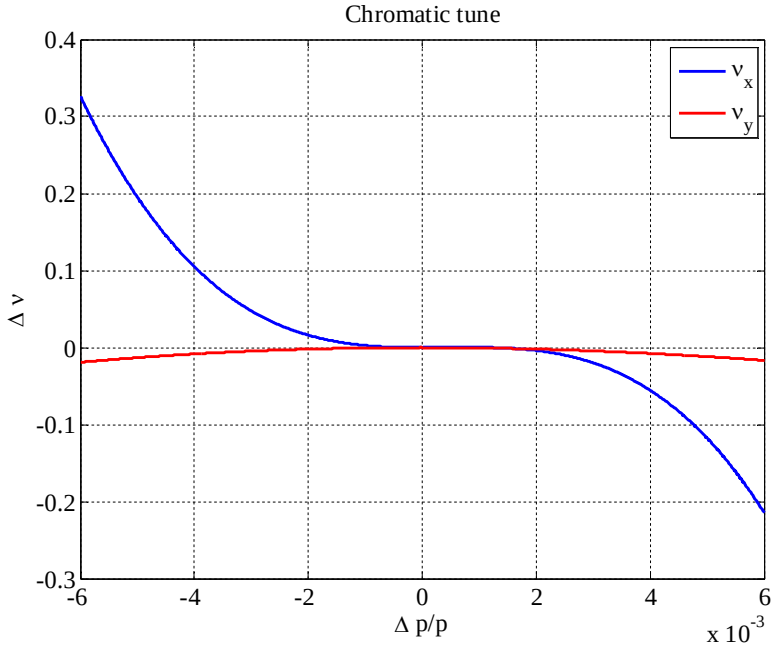

Figure 9. Chromatic tune shift for the ring with IR local sextupole pairs and three families of arc sextupoles. The horizontal chromatic tune shift is dominated by a large 3rd order term.

FURTHER COMPENSATION OF NON-LINEAR EFFECTS

Dynamic aperture simulations with the implemented local IR chromaticity correction revealed that the vertical dynamic aperture is not sufficient, likely due to the large vertical amplitude dependent tune shift (see Fig. 8). Secondly, the range of stable off-momentum motion is limited to $\Delta p/p = 0.4\%$ due to large horizontal chromatic tune shift (Fig. 9). In order to improve the dynamic aperture, additional orthogonal non-linear correction systems (knobs) were added in the IR. These include (per half-IR): 1) one octupole (OCT1) at a non-dispersive location with large vertical beta function to correct the vertical amplitude dependent tune shift; 2) a pair of weak sextupoles placed symmetrically around each main SIRY1 and SIRY2 sextupoles to compensate the effect of the finite sextupole length (the latter is amplified by the very high beta function); and 3) a –I pair of opposite polarity octupoles (OCT2) near the main SIRX1, SIRX2 sextupoles (where β_x and dispersion are large) to correct the 3rd order horizontal chromatic tune shift. Positions of these sextupoles and octupoles in the IR are shown in Fig. 10. More detailed description of these correction knobs is given below.

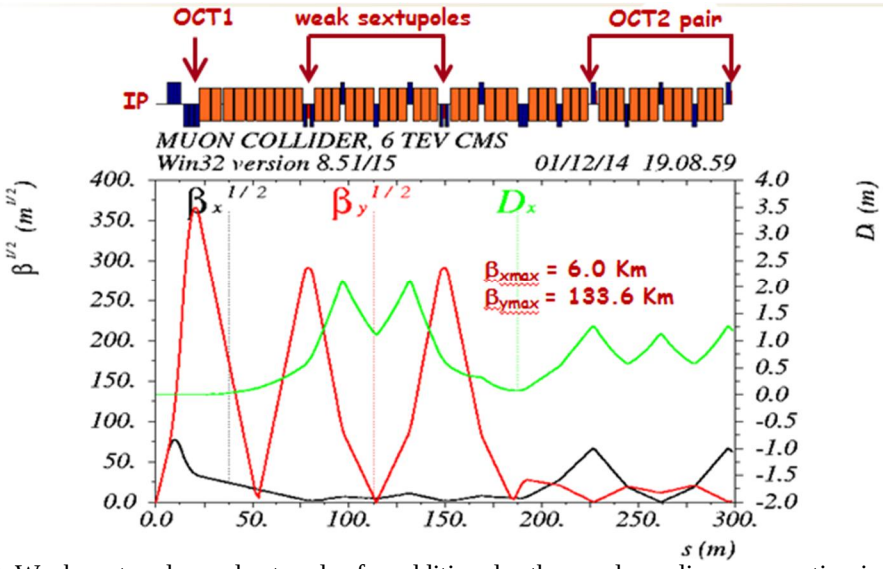

Figure 10. Weak sextupoles and octupoles for additional orthogonal non-linear correction in the IR.

Correction of Vertical Amplitude Dependent Tune

A thin length octupole (OCT1) is included on the outer side of each FF doublet for control of vertical tune shift with vertical amplitude. Due to the large β_y/β_x ratio at this location, the octupole effect is mostly in the vertical plane. Additionally, due to the zero dispersion, the OCT1 does not create chromaticity. Hence, such an octupole can be used as an orthogonal knob for tuning the vertical tune shift with amplitude. The integrated strength of the octupole $K_3L = 0.01031\ m^{-3}$ was initially determined using LEGO by minimizing the vertical tune shift with vertical amplitude, where $K_3 = \frac{B'''}{6B\rho}$, L is the effective length, and Bρ the magnetic rigidity. This setting improved the on-momentum vertical dynamic aperture, but the off-momentum aperture was still insufficient, as shown in Fig. 11. As a second step, the octupole strength was optimized in LEGO to maximize the vertical dynamic aperture for both on and off-momentum particles, as shown in Fig. 12. In this case, the optimal octupole strength is $0.022\ m^{-3}$. The amplitude dependent tune shifts with and without octupole correction are compared in Table 3. One can notice that in order to improve the off-momentum dynamic aperture the vertical tune shift with vertical amplitude is driven to a larger value with opposite sign. Also, the vertical tune shift with the horizontal amplitude changes sign as well. In combination, these two terms result in a different orientation of the tune footprint as can be seen in Fig. 13 and in the plot of the tune shift derived from tracking in Fig. 14. The latter shows that the vertical tune with amplitude is driven

away from the integer resonance, thus increasing the vertical dynamic aperture as compared to Fig. 6 without the OCT1. The impact of OCT1 on the horizontal tune shift is small confirming that the octupole effect is primarily in the vertical plane. Although, the OCT1 adjustment improves the overall dynamic aperture, the off-momentum range is still limited to 0.4%. This is likely due to the large 3rd order horizontal chromatic tune shift which needs to be reduced.

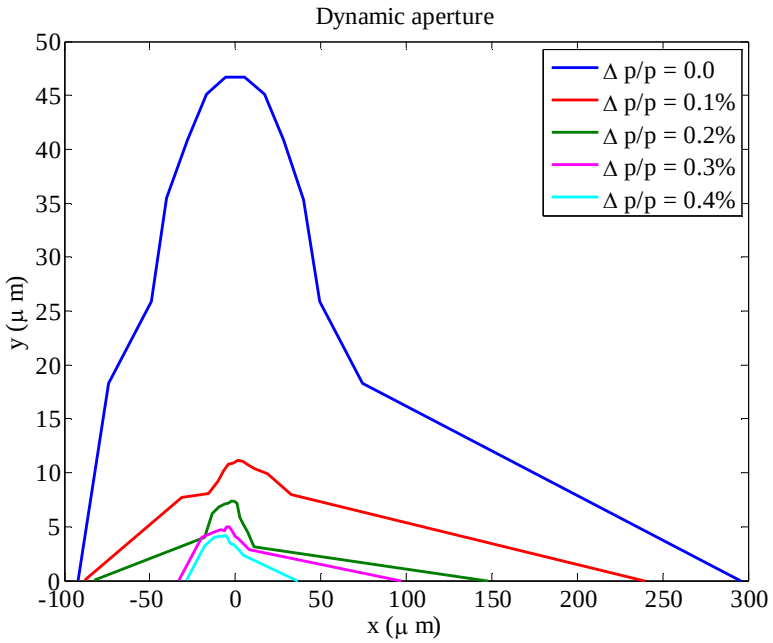

Figure 11. Dynamic aperture for the initial setting of the OCT1 integrated strength of 0.01031 m^{-3}. Only the on-momentum aperture is improved.

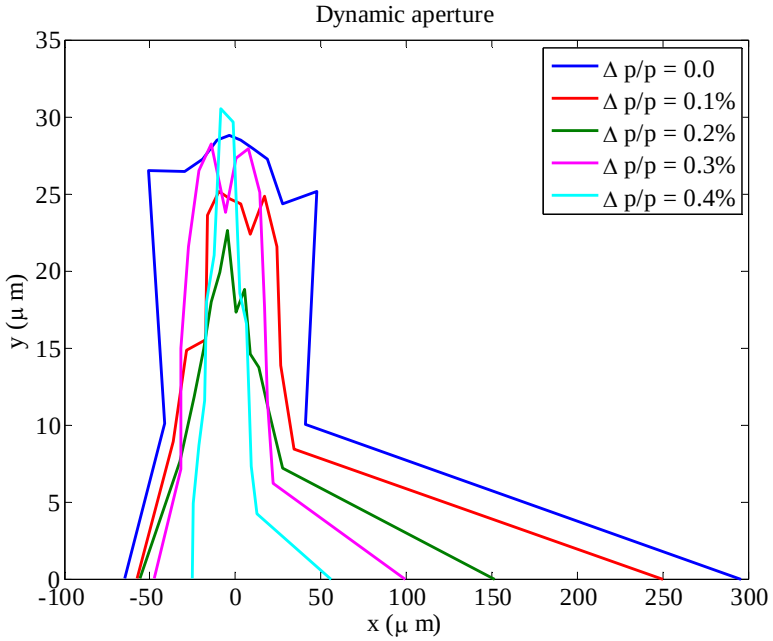

Figure 12. Dynamic aperture with the optimized OCT1 strength of 0.022 m^{-3}. The on and off-momentum apertures are improved, but the momentum range is limited to $\Delta p/p = 0.4\%$.

Table 3. Tune shift with amplitude versus OCT1 strength.

K_3L, m^{-3}	d(Qx)/d(Jx)	d(Qy)/(dJy)	d(Qy)/d(Jx)
0.0	5.61E+03	-1.33E+07	4.88E+04
0.01031	6.56E+03	4.23E+03	-1.77E+05
0.022	7.63E+03	1.52E+07	-4.33E+05

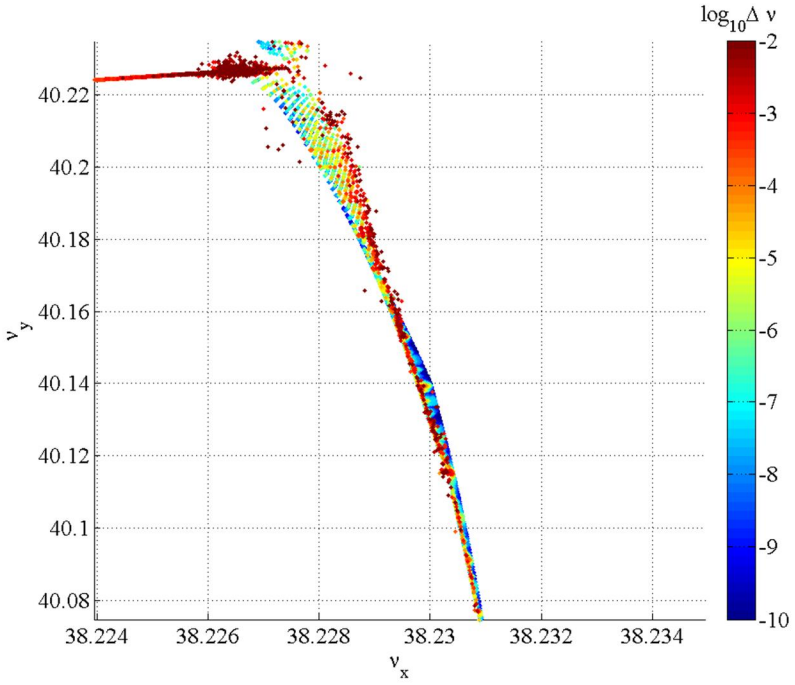

Figure 13. Tune footprint with the optimal OCT1 strength of 0.022 m^{-3}. The vertical tune shift with horizontal amplitude changes sign as compared to Fig. 7.

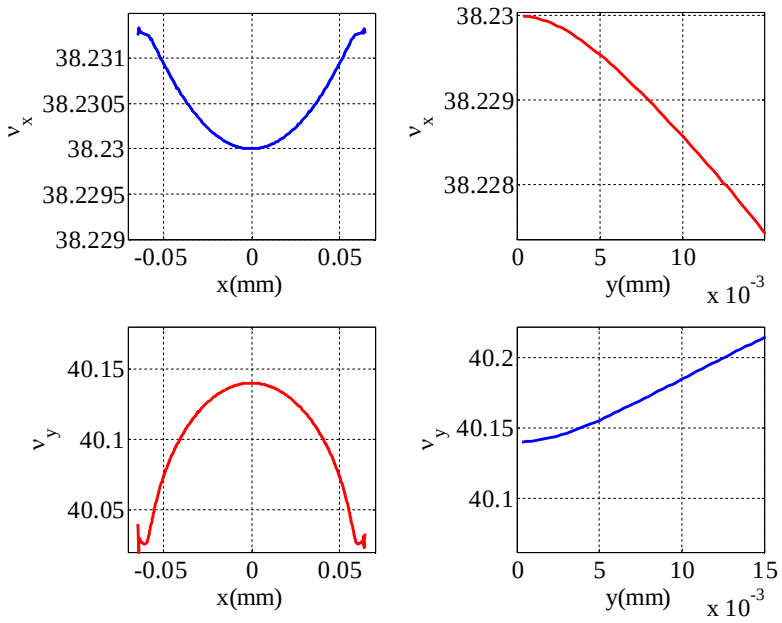

Figure 14. Tune shift with amplitude with the optimal OCT1 strength of 0.022 m^{-3}. The vertical tune shifts with vertical and horizontal amplitude change sign as compared to Fig. 8. The octupole effect on the horizontal tune shift is very small.

Correction of the Effect of Finite Sextupole Length

Cancellation of non-linear geometric effects caused by sextupoles in a –I pair is exact only in the approximation of a thin sextupole (i.e. for zero sextupole length). For realistic sextupoles with non-zero length the residual effects can be significant if beta functions at the sextupoles are very large such as at the SIRY1 and SIRY2 sextupoles. Fig. 15 shows dynamic aperture when the SIRY1,2 are modelled as thin sextupoles (octupoles are off). In this case, the on-momentum aperture is very large as compared to the case with thick sextupoles in Fig. 6. Table 4 shows that the vertical tune shift with the vertical amplitude is reduced and changes sign in case of the thin sextupoles, while the other tune shift terms remain almost unchanged.

Table 4. Amplitude dependent tune shift for thin and thick model of SIRY1,2 sextupoles (octupoles off).

	d(Qx)/d(Jx)	d(Qy)/(dJy)	d(Qy)/d(Jx)
Thick SIRY1,2	5.61E+03	-1.33E+07	4.88E+04
Thin SIRY1,2	5.61E+03	2.10E+06	4.88E+04

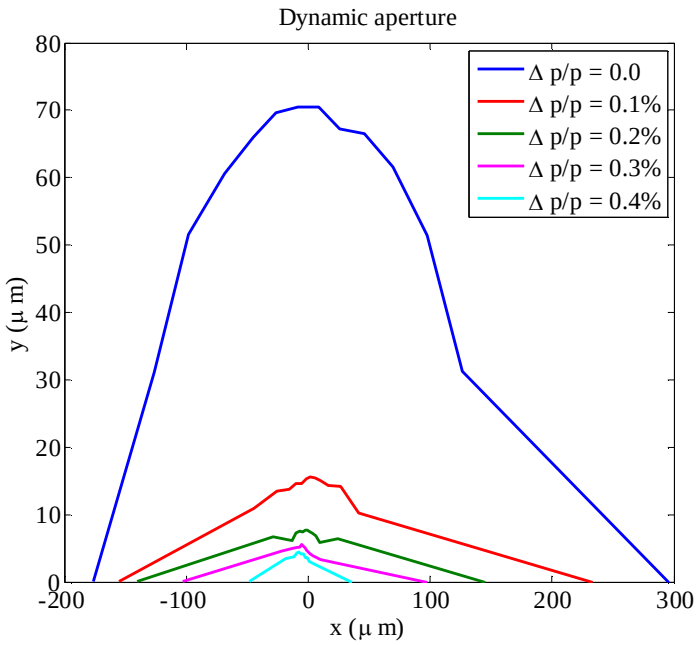

Figure 15. Dynamic aperture with thin SIRY1,2 sextupoles (octupoles are off).

It was shown previously [12] that the non-linear effect of the finite sextupole length can be reduced by adding a –I pair of weak sextupoles to each main –I sextupole pair, where a weak sextupole is placed near the corresponding main sextupole. This method, however, provides only partial compensation. An improved version of such correction [13] requires the use of two pairs of weak sextupoles (instead of one) per each –I pair of the main sextupoles. In this case, each main sextupole is accompanied by two weak correcting sextupoles placed symmetrically on either side of the main sextupole. The four weak sextupoles, therefore, form two –I pairs as can be seen in the schematic layout in Fig. 16, where S1 and S2 are the strengths of the main and the weak sextupoles, L is the sextupole length, and kL is the distance between the main and the weak sextupoles. The strength S2 required for compensation of the effect of the finite sextupole length (up to the order of L^5) is determined by the equation: $2(7 + 6k)(\frac{S2}{S1})^2 + 12(1 + k)\left(\frac{S2}{S1}\right) + 1 = 0$ [13]. Using k = 0.5 and choosing the solution with a weaker S2, the resulting ratio of S2/S1 is -0.0595. The corresponding dynamic aperture, where the weak sextupoles are correcting the SIRY1,2 sextupoles, is shown in Fig. 17 (with octupoles off). One can see that the resulting aperture is very similar to the one with thin sextupoles in Fig. 15. This, therefore, confirms that the above correction, indeed, compensates the effect of the finite length of the SIRY1,2 sextupoles.

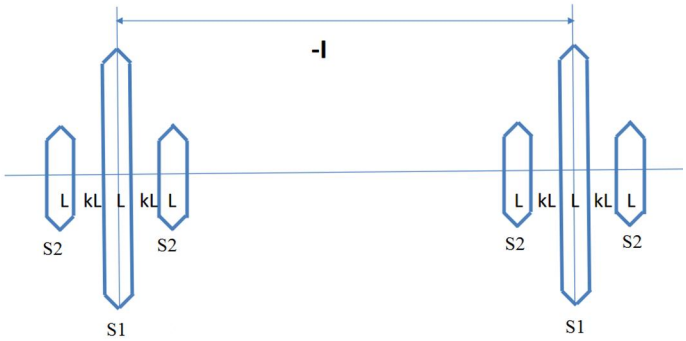

Figure 16. Schematic layout of weak sextupoles for correction of the effect of finite sextupole length, where S1 and S2 are the strengths of the main and weak sextupoles, L is the sextupole length, and kL is the distance between the main and the weak sextupoles.

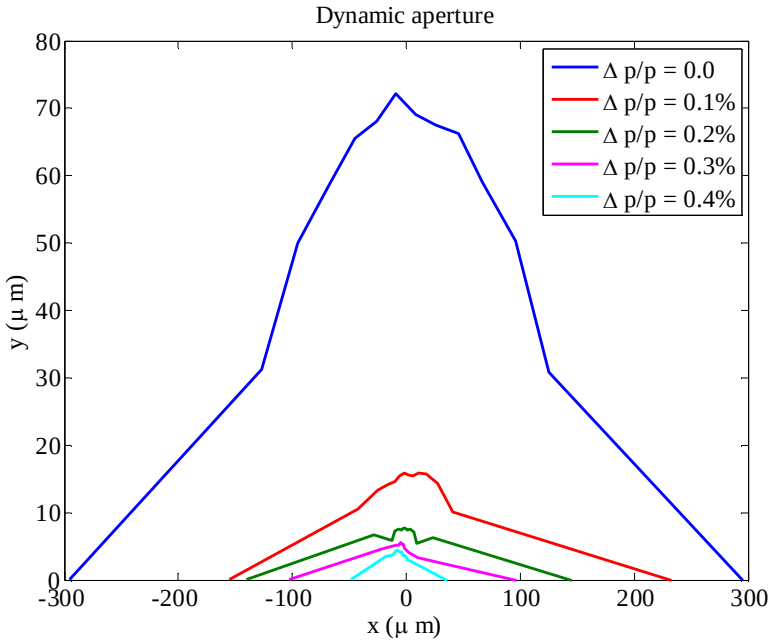

Figure 17. Dynamic aperture with the corrected effect of finite sextupole length (with octupoles off). The ratio of S2/S1 is -0.0595. The on-momentum dynamic aperture is similar in size to the one with thin length sextupoles in Fig. 15.

Further improvement was achieved when the OCT1 octupoles were included in addition to the above weak sextupole correction. The octupole strength was re-optimized to 0.0147 m^{-3} to maximize the on and off-momentum dynamic aperture - see Fig. 18. The momentum range in this case is still limited to 0.4%.

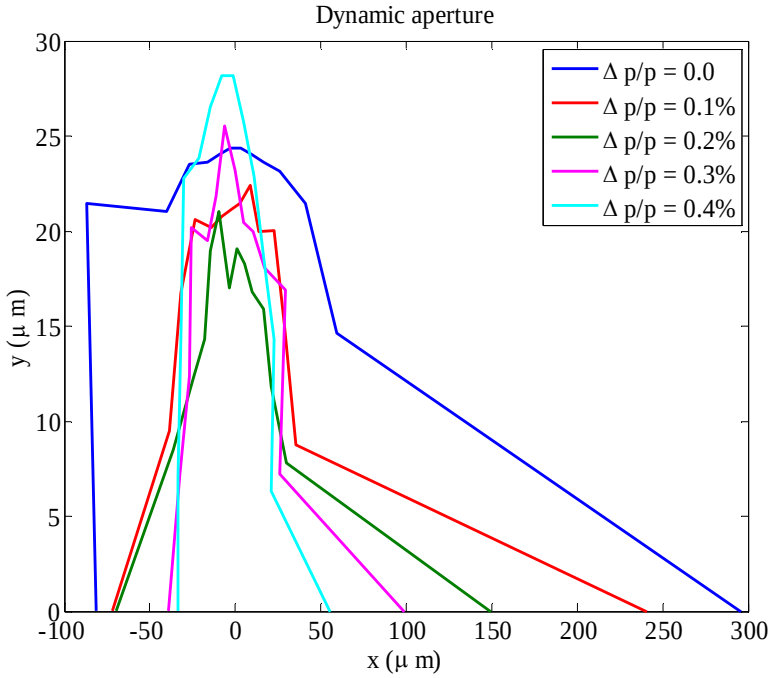

Figure 18. Dynamic aperture with the correction of the finite sextupole length effects and with the OCT1 strength of 0.0147 m^{-3}.

Correction of Horizontal Chromatic Tune Shift

Fig. 9 shows that the large horizontal chromatic tune shift is dominated by a cubic term which may be the limiting factor for the observed dynamic aperture momentum range. To correct this term, a –I pair of thin length octupoles (OCT2) is added next to the –I pair of the main IR horizontal sextupoles SIRX1,2 where dispersion is sufficiently large. The two octupoles in this pair have opposite polarities in order to cancel the octupole contributions to the horizontal amplitude dependent tune shift and to the quadratic term of the horizontal chromatic tune shift. Due to the large β_x/β_y ratio at this location, these octupoles mostly affect the horizontal plane, thus providing an orthogonal correction. Fig. 19 shows that the OCT2 can effectively control the 3rd order term of the horizontal chromatic tune shift. For the OCT2 pair strength of $K_3L = \pm 14.5$ m^{-3}, the corresponding dynamic aperture is shown in Fig. 20. In this case, the weak sextupoles and OCT1 octupoles were turned off causing relatively small vertical aperture; however, the momentum range is increased to 0.5% due to the corrected horizontal chromatic tune shift. The final optimized dynamic aperture including the weak sextupoles and OCT1, OCT2 octupole correction knobs is shown in Fig. 21. One can see that the on-momentum aperture is large (8σ), and the off-momentum aperture is above or close to 5σ for the momentum range of up to 0.5%.

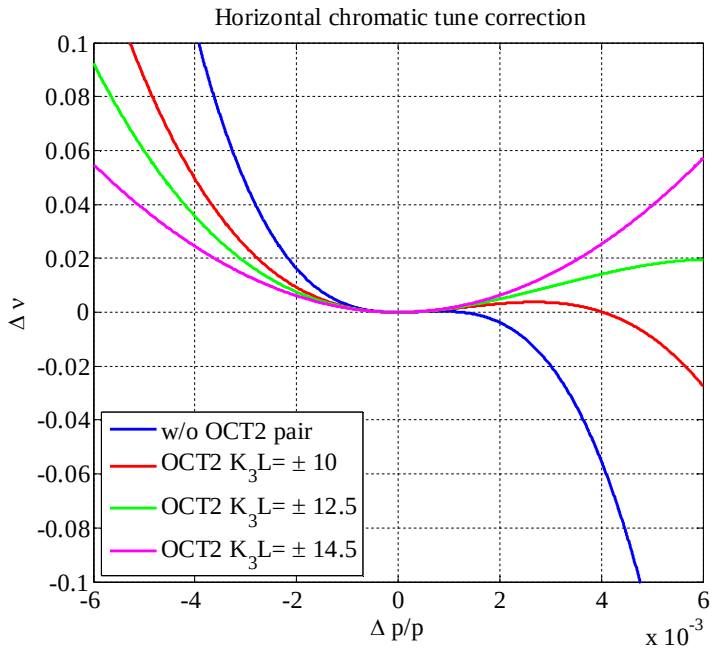

Figure 19. Horizontal chromatic tune shift as a function of OCT2 strength.

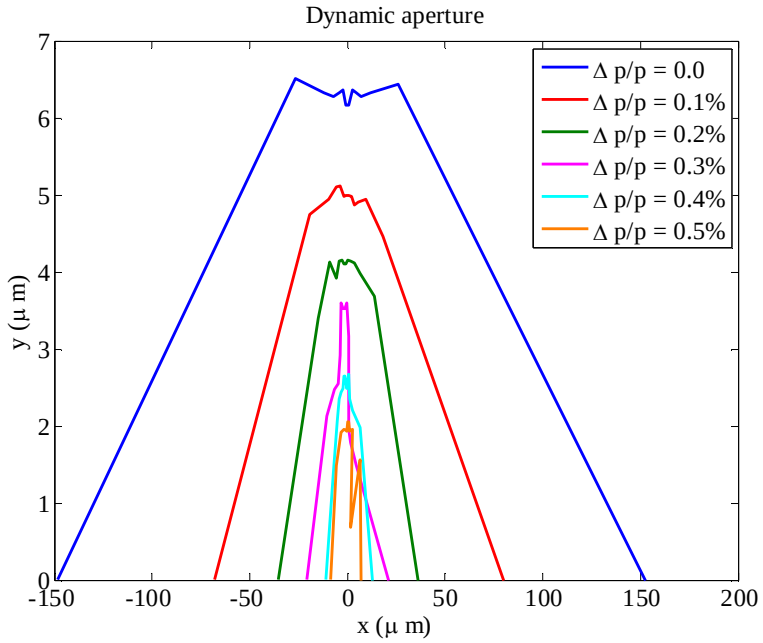

Figure 20. Dynamic aperture with the corrected horizontal chromatic tune shift, where the strength of OCT2 octupoles is set to 14.5 m^{-3} (OCT1 octupoles and weak sextupoles are off). The momentum range is increased to 0.5%.

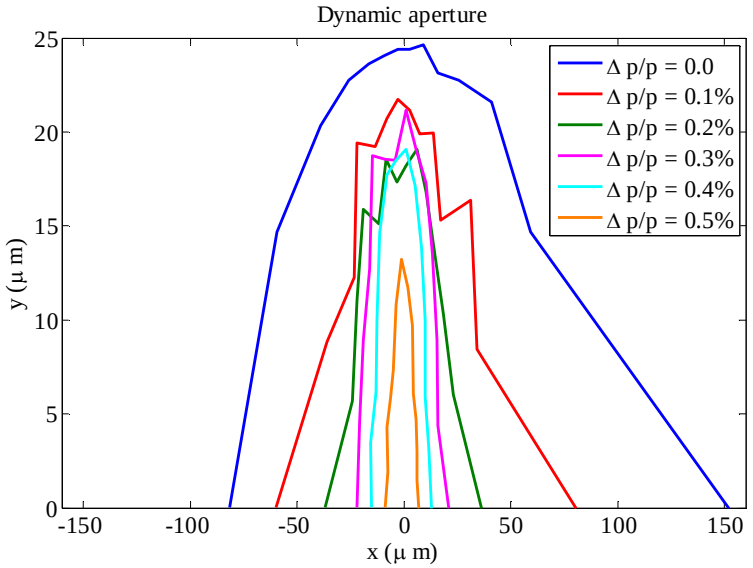

Figure 21. Final optimized dynamic aperture with the OCT1 strength of 0.0147 m^{-3}, the OCT2 pair strength of ±14.5 m^{-3}, and the weak sextupole correction.

CONCLUSION

The lattice design of a muon collider ring with 6 TeV CM energy and circumference of 6.3 km is presented. The very high beta functions in the FF quadrupoles cause strong non-linear chromatic aberrations limiting the dynamic aperture. To minimize these effects, we include non-interleaved –I pairs of IR sextupoles for local chromaticity correction as well as additional pairs of IR weak sextupoles and two families of octupoles to compensate the 3rd order horizontal chromatic tune shift, the non-linear effects of finite length of the IR sextupoles, and the vertical

amplitude dependent tune shift. Additionally, the arc lattice is designed for cancellation of most sextupole driven resonance driving terms in each half-arc. Optimization of the above non-linear corrections results in sufficient dynamic aperture within the momentum range of ±0.5%.

ACKNOWLEDGEMENTS

Authors would like to thank Dr. Y. Alexahin for providing the lattice for 1.5 TeV CM muon collider ring and the reference materials.

REFERENCE

[1] E. Eichten," Future High Energy Colliders", MAP Spring Meeting, FNAL, USA (2014).

[2] Y. Alexahin, et al., "Muon Collider Lattice with Local Interaction Region Chromaticity Correction", Proceedings of PAC09, Vancouver, BC, Canada, pp. 3820-3822 (2009).

[3] N.V. Mokhov, A.V. Van Ginneken, Proceedings of ICRS-9, Tsukuba, Japan, 1999; J. Nucl. Sci. Techn., pp.172-179 (2000).

[4] Y. Alexahin, private communication.

[5] Y. Alexahin, et al., "A 3-Tev Muon Collider Lattice Design", Proceedings of IPAC2012, New Orleans, Louisiana, USA, pp. 1254-1256 (2012).

[6] Y. Alexahin, et al., "Muon collider interaction region design", PRST-AB 14, 061001 (2011).

[7] M-H Wang, et al., "SLAC effort in the collider design", MAP 2014 Spring Meeting, FNAL, USA (2014).

[8] Y. Cai, et al., "Ultimate Storage Ring Based On Fourth-Order Geometric Achromats", Phys. Rev. ST Accel. Beams 15, 054002 (2012).

[9] K. L. Brown and R. V. Servranckx, "Optics modules for circular accelerator design", Nucl. Instrum. Methods Phys. Res., Sect. A 258, 480 (1987).

[10] H. Grote and F.C. Iselin, "The MAD Program User's Reference Manual", CERN/SL/90-13 (AP).

[11] Y. Cai, M. Donald, I. Irwin, Y. Yan, "LEGO: A Modular Accelerator Design Code", SLAC-PUB-7642.

[12] A. Bogomyagkov, et al., "Effect of the Sextupole Finite Length on Dynamic Aperture in the Collider Final Focus", arXiv:0909.4872v1 (2009).

[13] Y. Cai, "Optics with Large Momentum Acceptance for Higgs Factory", Future Circular Collider Kick-off Meeting, Geneva, Switzerland (2014).